

12B.1 Evaluation of GEM in the Stable Boundary Layer over the Arctic Ocean during SHEBA

Pierre-Luc Carpentier*, Colin Jones
University of Quebec at Montreal, Canada

1. Introduction

Most Coupled Global Climate Models (CGCMs) project an important amplification of climate change in the atmospheric boundary layer over the Arctic Ocean during the 21st century when they are forced with increasing concentration of atmospheric CO₂ (IPCC, 2007; Holland and Bitz, 2003). However, the models disagree considerably on the amplitude of the projected amplification since the inter-model spread is larger in the Arctic than anywhere on the planet. Part of the arctic climate system sensitivity could be due to surface feedbacks involving important processes involved in the surface heat budget, such as radiation and turbulence. Feedback involving these processes could significantly amplify the local climate change signal and reduce dramatically the volume of sea-ice in the Arctic Ocean.

Turbulent fluxes of heat, momentum and moisture play a critical role in the atmosphere-ice-ocean interaction by affecting the surface heat budget, cloud cover and sea-ice drift. Consequently, errors made in the simulation of turbulent processes may reduce the level of confidence in climate projections. According to Tjernström *et al.* (2004), important errors are made by models participating in the Arctic Regional Climate Model Intercomparison Project (ARCMIP) when simulating the stable boundary layer. For example, the latent heat flux is significantly overestimated by all six ARCMIP models. Such errors could potentially trigger a feedback in the models by inducing an overestimate of cloud cover and radiation effects. Consequently, modeling errors introduced by the parameterization of key surface processes may reduce the level of confidence in climate projections.

The aim of this project is to evaluate the ability of the Global Environmental Multi-Scale (GEM) model (Côté *et al.*, 1998) to represent turbulent processes and near-surface state variables in the stable

boundary layer, observed during the Surface Heat Budget of the Arctic Ocean (SHEBA) experiment (Uttal *et al.*, 2002).

2. Model experiment

A simulation was made with GEM using a limited area grid of 70x80 grid boxes centered at a longitude of 156°W and a latitude of 67°N with a horizontal resolution of 0.5° (Figure 1). 53 vertical levels were used with the top of the model located at 10 hPa. The model integration began in September 1996 and ended in October 1998, with a 30 minutes time step. A spin-up period of one year was included before comparing GEM with the SHEBA observations made in the Beaufort Sea, that started in October 1997 and ended a year later. Lateral boundary conditions were supplied from ERA-40 every 6 hours and the surface boundary conditions of ice fraction and sea-surface temperature (SST) were prescribed from the AMIP II dataset. Contrary to the ARCMIP experiment set up, sea-ice temperature was calculated in the GEM integration.

To evaluate GEM we make extensive use of the SHEBA main tower observations, at five levels (ranging from 2 to 18 meters high), of turbulent fluxes, flux-profile relationships and bulk Richardson number. The main tower was installed over sea-ice in the Beaufort Sea for a full annual cycle (Persson *et al.*, 2002; Grachev *et al.*, 2008). Observations from the Ice Physics Group at SHEBA are also used (Perovich *et al.*, 2001).

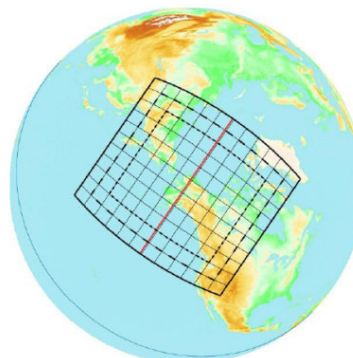


Figure 1. Limited area domain used in this research project. The GEM model was run with an horizontal resolution of 0.5°.

* Corresponding author address: Pierre-Luc Carpentier, Ouranos, 550 Sherbrooke West, 19th floor, Montreal, Qc, Canada, H3A 1B9, (514)282-6464, ext. 315, carpentier.pierre-luc@sca.uqam.ca

3. Results

a) Surface fluxes and state variables

Comparisons of simulated near-surface state variables with SHEBA observations are shown in Figures 2 and 3. The surface wind comparison (Figure 2) suggests large errors occur under calm conditions, with GEM systematically overestimating the wind speed by an average of 0.95 m/s for all conditions observed during the SHEBA year. Also, the model does not simulate wind speeds below 1.6 m/s because of a minimum value imposed on the stability calculation.

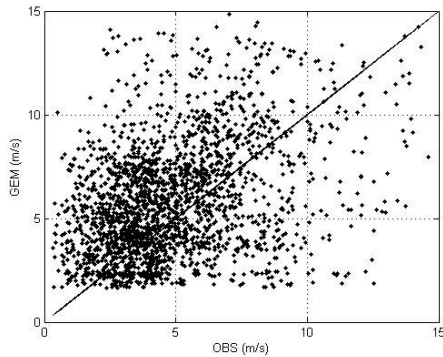
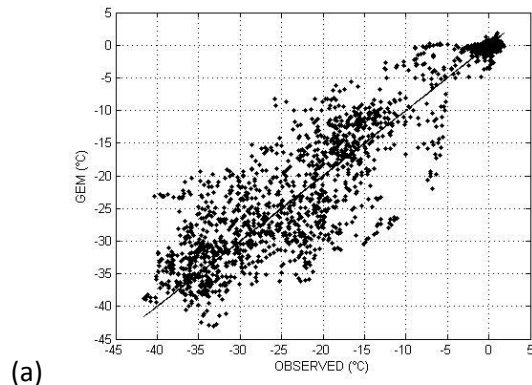
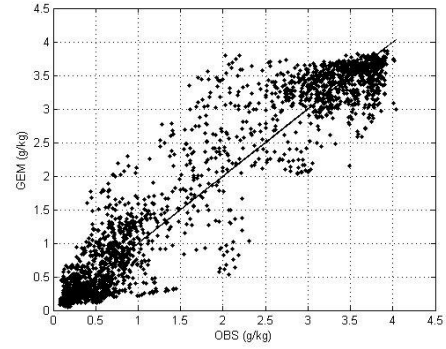


Figure 2. Scatter plots of observed (horizontal axis) versus modelled (vertical axis) near-surface wind. The scatter plots are based on 3 hourly mean time series for the October 29th 1997–October 1st 1998 period.

Surface air temperature and specific humidity (Figures 3a and 3b respectively) are reasonably well simulated, considering that sea-ice surface temperature was not prescribed in the model. Temperature errors are lower in summer as they are constrained around 0°C during the melt season. GEM has an overall warm bias of 0.62°C in comparison with SHEBA observations.



(a)



(b)

Figure 3. Same as Figure 2 for (a) 2-meter temperature and (b) 2-meter specific humidity.

The comparison of simulated surface turbulent fluxes with SHEBA observations (Figures 4 to 6) show that like most of the ARCMIP models, GEM overestimates the friction velocity (momentum flux) with a bias of 0.06 m/s for all conditions, with the largest errors during calm conditions. Such conditions are generally associated with very weak surface winds, cold surface temperature and an intense near-surface temperature inversion. Many models deliberately use enhanced momentum mixing on purpose in such conditions in order to prevent decoupling of the surface that may lead to runaway cooling (Derbyshire, 1998; Cuxart *et al.*, 2005). It is likely that GEM overestimates mixing in calm conditions for the same reason.

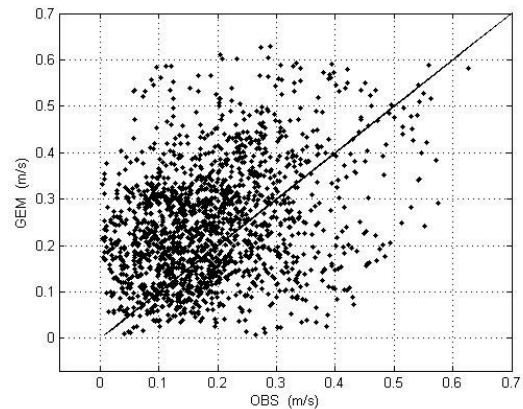


Figure 4. Same as Figure 2 for friction velocity.

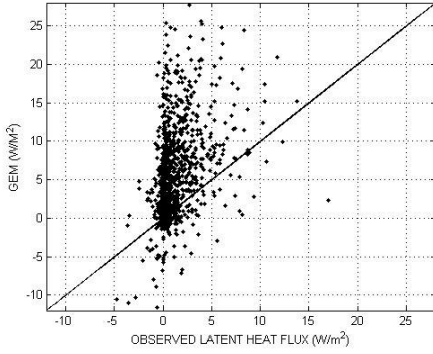


Figure 5. Same as Figure 2 for latent heat flux. Positives fluxes are in the upward direction.

Large errors are found for the simulated latent heat flux (Figure 5). Similar to the ARCMIP models (Tjernström *et al.*, 2004), the latent heat flux exhibits a large positive bias (of 3.84 W/m^2) in GEM. Even if the latent heat flux amplitude is small compared with the other components of the surface heat budget, such errors could lead to an overestimation of the low-level cloud cover by an erroneous vertical transport of moisture. Consequently, the surface heat budget could be indirectly affected.

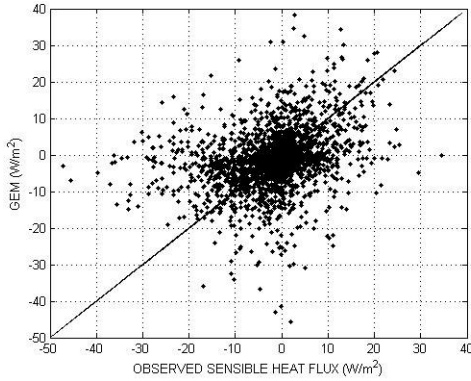


Figure 6. Same as Figure 2 for sensible heat flux. Positive fluxes are in the upward direction.

The observed mean sensible heat flux is -1.92 W/m^2 while the mean simulated flux is -1.66 W/m^2 (Figure 6). The amplitude of the flux is reasonable in comparison with the latent heat flux.

b) Surface fluxes as a function of stability

Figures 7 to 9 show the observed and simulated relationship between surface turbulent fluxes and stability quantified in GEM by the inverse of Obukhov length

$$\frac{1}{L} := -\frac{\kappa g (\overline{w'\theta'_v})_s}{\bar{\theta}_{vs} u_*^3} \quad (1)$$

where κ is the von Karman constant, $(\overline{w'\theta'_v})_s$ is the virtual potential temperature flux at the surface, g is the gravitational acceleration. In GEM, the friction velocity u_* is calculated by

$$u_*^2 := -(\overline{u'w'})_s = C_m \bar{V}_r^2 \quad (2)$$

where $(\overline{u'w'})_s$ is the turbulent flux of momentum at the surface. Figure 7 shows the important effect stability has on the friction velocity. As stability increases, mixing is damped very efficiently by the temperature inversion in the observations. GEM captures this feature reasonably well.

The sensible heat flux intensity calculated by

$$\rho C_p (\overline{w'\theta'_v})_s = -C_h \bar{V}_r (\bar{\theta}_{vr} - \bar{\theta}_{vs}) \quad (3)$$

where C_h is the transfer coefficient for heat, $\bar{\theta}_{vr}$ is the potential temperature at 2 meters and $\bar{\theta}_{vs}$ is the surface potential temperature. Figure 8 shows the simulated and observed relationship between the sensible heat flux and stability. Contrary to the friction velocity, the sensible heat flux is enhanced as stability increases in the weakly stable regime. A maximum value of -60 W/m^2 is reached when the Obukhov length is approximately 1000 meters in the observations and 100 meters in GEM. For the very stable regime ($L > 100$ meters), the sensible heat flux decreases as stability increases. This effect is also relatively well simulated by the model.

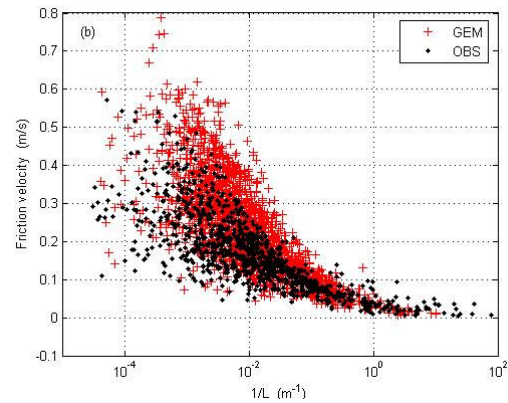


Figure 7. Friction velocity as a function of stability expressed by the inverse of Obukhov length in stable stratification. The dataset used is based on 3 hourly mean time series for the October 29th 1997–October 1st 1998 period.

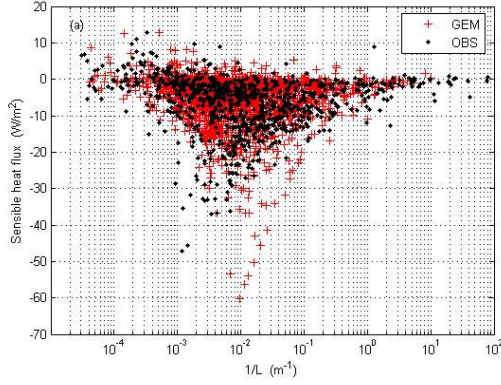


Figure 8. Same as Figure 7 for sensible heat flux in stable stratification. Positive fluxes are in the upward direction.

The latent heat flux is calculated by

$$\rho L_s \overline{(w'q_v')}_s = -C_v \bar{V}_r (\bar{q}_{vr} - \bar{q}_{vs}) \quad (4)$$

where C_v , equal to C_h in the default configuration of GEM, is the transfer coefficient for moisture, \bar{q}_{vr} is the specific humidity at 2 meters and \bar{q}_{vs} is the surface specific humidity saturated at $\bar{\theta}_{vs}$. The variation of the observed surface latent heat flux as a function of stability is different from the simulated relationship in many ways. First, the latent heat flux is generally overestimated by GEM. Also, in GEM a maximum of negative fluxes at $L = 100$ meters is absent from the observations.

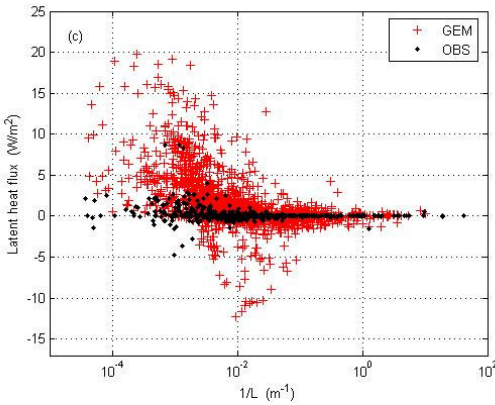


Figure 9. Same as Figure 7 for latent heat flux. Positive fluxes are in the upward direction.

c) Impact of latent heat flux overestimation

A sensitivity analysis was made in order to quantify the potential impact of the large overestimate of the latent heat flux in GEM. The model was rerun using a

new drag coefficient for moisture that is different from the drag coefficient for heat such that $C_v = C_h/\beta$ where β is a constant equal to 5.0. This parameterization was designed in order to agree better with the SHEBA observations (see Figure 10). Consequently, we expect the new run results to be more realistic.

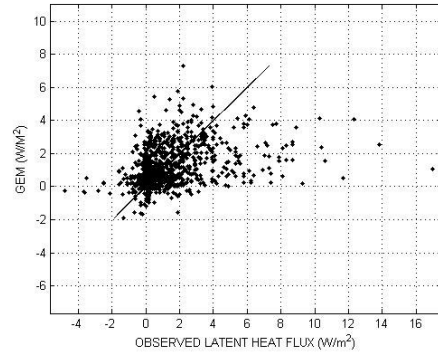


Figure 10. Comparison of observed and modelled latent heat flux using $C_v=C_h/5$.

The new results obtained with this change are shown in Figures 11 to 17. A new comparison of simulated against observed latent heat flux is shown in Figure 11. Not surprisingly, the simulated latent heat flux is much smaller than the one shown in Figure 5 since the drag coefficient is now five times smaller.

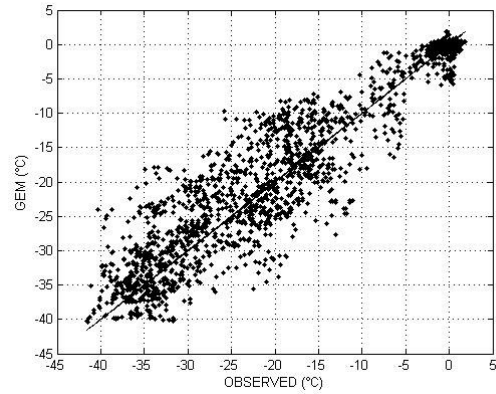


Figure 11. Comparison of observed and modelled surface air temperature using $C_v=C_h/5$.

The new comparison of surface air temperature shown on Figure 11 has a lower root mean square error than originally while the bias is similar to the default configuration. On the other hand, cloud

cover was systematically lower during the whole SHEBA year as shown on Figure 12 probably because of the decrease in vertical transport of moisture when $C_v=C_h/5$.

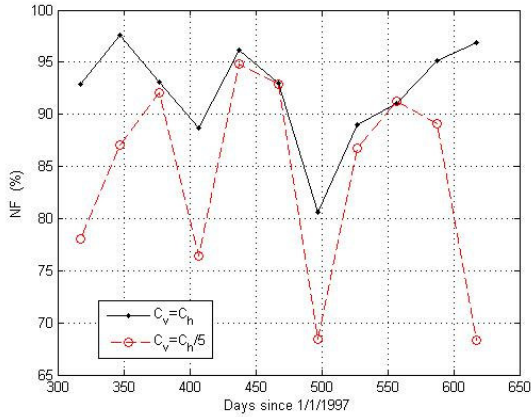


Figure 12. Monthly mean cloud cover simulated at the SHEBA point compared for the two configurations.

Sea-ice and snow thickness evolution are shown on Figures 13 and 14 for the full annual cycle. The original run made with the default configuration of GEM ($C_v = C_h$) is compared with the results obtained with the new formulation ($C_v = C_h / 5$) on this Figure. The reduction in the latent heat flux intensity had the interesting effect of producing a thicker sea-ice and a thinner snow depth. The insulating effect of the snow cover could be responsible for this effect.

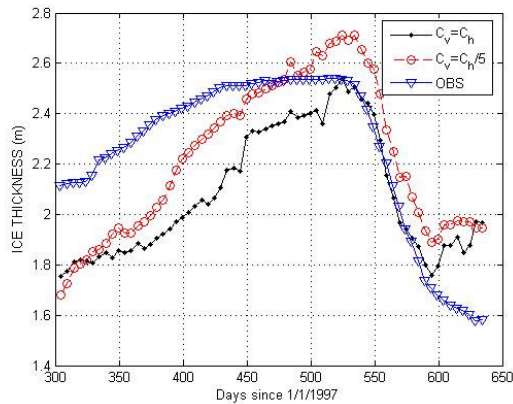


Figure 13. Simulated and observed 5 days mean sea-ice thickness at the SHEBA station.

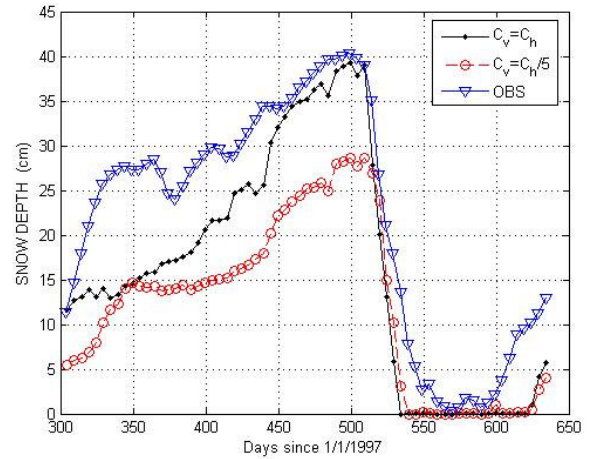


Figure 14. Simulated and observed 5 days mean snow depth at the SHEBA station.

The incoming shortwave radiation at the surface (Figure 15) is generally higher at the surface during the summer season for the low latent heat flux configuration. This effect is consistent with the fact that the cloud cover was systematically lower.

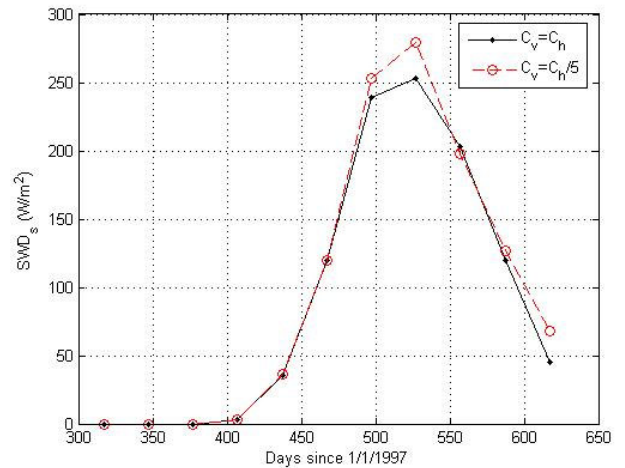


Figure 15. Simulated monthly mean incoming shortwave radiation at the surface for a full annual cycle.

A persistent decrease in the incoming shortwave radiation is also reported on Figure 16 where $C_v=C_h/5$.

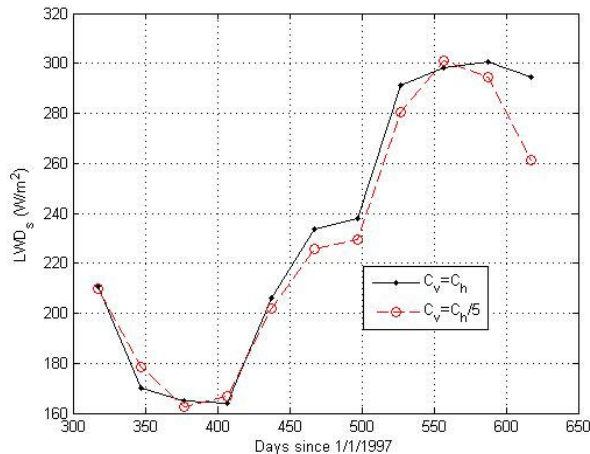


Figure 16. Simulated monthly mean incoming longwave radiation at the surface for a full annual cycle.

4. Discussion and Conclusion

The results obtained so far in this research project are suggesting that GEM with the default configuration is reasonably well compared with the other ARCMIP models for a very similar experiment. Large overestimation of the latent heat turbulent flux is also reported for the other ARCMIP models. Surface flux of momentum (friction velocity) is generally overestimated and large errors are found in calm conditions. Errors in surface fluxes simulation are also likely to exist in CGCMs runs since those models are using a very similar scheme based on bulk transfer formula. Also, the near-surface state variables are reasonably well simulated given the complexity of the problem.

The result obtained also highlights the potential indirect effect that the latent heat flux overestimation could have on the surface heat budget by affecting the cloud cover. It also suggests that the ice thickness and snow depth could be importantly affected by this type of error.

The sensitivity of the simulations to roughness length parameterization (e.g. Andreas *et al.*, 2005) will be evaluated in future work.

4. References

Andreas, E. L., Jordan, R. E., Makshtas, A.P., 2005: Parameterizing turbulent exchange over sea ice : The

ice station Weddell results. *Boundary-Layer Meteorol.*, **114** : 439-460.

Coté, J., Gravel, S., Méthot, A., Patoine, A., Roch, M., Staniforth, A., 1998 : The operational CMC-MRB global environmental multiscale (GEM) model: Part I- design considerations and formulation. *Mon. Wea. Rev.* , **126**, 1373-1395.

Cuxart, J., *et al.*, 2005: Single-column model intercomparison for a stably stratified atmospheric boundary layer. *Boundary-Layer Meteorol.*, **118** : 273-303.

Delage, Y., 1996: Parameterizing sub-grid scale vertical transport in atmospheric models under statically stable conditions. *Boundary-Layer Meteorol.*, **82** : 23-48.

Derbyshire, SH, 1998: Boundary-layer decoupling over cold surfaces as a physical boundary instability. *Boundary-Layer Meteorol.*, **90** : 297-325.

Grachev, A., Andreas, E. L., Fairall C.W., Guest, P. S., Persson, P. O. G., 2008 : Turbulent measurements in the stable atmospheric boundary layer during SHEBA : ten years after. *Acta Geophysica*, vol. **56**, no. 1., 142-166.

Holland, M. M., Bitz, C. M., 2003 : Polar amplification of climate change in coupled models. *Clim. Dyn.*, **21** : 221-232.

Perovich, D.K., Grenfell, CG, Richter-Menge, JA, Light, B., Tucker, WB, Eicken, H, 2001 : Thin and thinner: Sea ice mass balance measurements during SHEBA. *J. Geophys. Res.*, **108**(C3), 8050.

Persson, P. O. G., Fairall, CW, Andreas, EL, Guest, PS, Perovich, DK, 2002 : Measurements near the Atmospheric Surface Flux Group tower at SHEBA : Near-surface conditions and surface energy budget. *J. Geophys. Res.*, **107**(C10), 8045.

Tjernström, M., *et al.*, 2004 : Modelling the arctic boundary layer : an evaluation of six ARCMIP regional scale models using data from the SHEBA project. *Boundary-Layer Meteorol.*, **117** : 337-381.

Uttal, T., *et al.*, 2002 : The surface heat budget of the Arctic Ocean. *Bull. Am. Meteorol. Soc.*, **83**, 255-275.